Printed light-trapping nanorelief Cu electrodes for full-solution-processed flexible organic solar cells

Kan Li[1,2], Yaokang Zhang[1,3], Hongyu Zhen[1,2], Liyong Niu[1,3], Xu Fang[2], Zhike Liu[4], Weidong Shen[2], Haifeng Li[2] and Zijian Zheng[1,3,*]

Dr. Kan Li, Mr. Yaokang Zhang, Dr. Hongyu Zhen, Mr. Liyong Niu, Prof. Zijian Zheng
1. Nanotechnology Center, Institute of Textiles and Clothing, the Hong Kong Polytechnic University, Hong Kong, China

E-mail: tczzheng@polyu.edu.hk

Dr. Kan Li, Dr. Hongyu Zhen, Mr. Xu Fang, Prof. Weidong Shen, Prof. Haifeng Li
2. State Key laboratory of modern optical instrumentation, Zhejiang University, 38# Zheda Road,Hangzhou 310027, P.R.China,

Mr. Yaokang Zhang, Mr Liyong Niu, Prof. Zijian Zheng
3. Advanced Research Centre for Fashion and Textiles, the Hong Kong Polytechnic University Shenzhen Research Institute, Shenzhen 518000, China

Dr. Zhike Liu
4. Department of Applied Physics, the Hong Kong Polytechnic University, Hong Kong, China

Keywords: printable, Cu electrodes, solution processed, flexible organic solar cells, polymer-assisted metal deposition

Abstract: Light-trapping nanorelief metal electrodes have been proven to be an effective approach to improve the absorption performance for flexible organic solar cells (FOSCs). These nanorelief electrodes have been made by conventional vacuum deposition techniques, which are difficult to integrate with roll-to-roll fabrication process. To address this challenge, this paper reports, for the first time, the fabrication of highly conductive nanorelief Cu electrodes on the flexible substrates through solution printing and polymer-assisted metal deposition at room temperature in the air. FOSCs made with these printed nanorelief Cu electrodes possess not only much improved power conversion efficiency by 13.5%, but also significant enhancement in flexibility when compared with those made with flat Cu electrodes. Because of the low material and fabrication cost, these printed nanorelief Cu electrodes show great promise in roll-to-roll fabrication of FOSCs in the future.

Li, K., Zhang, Y., Zhen, H., Niu, L., Fang, X., Liu, Z., ... & Zheng, Z. (2016). Printed light-trapping nanorelief Cu electrodes for full-solution-processed flexible organic solar cells. Materials Research Express, 3(7), 074006.

1. Introduction

Flexible organic solar cells (FOSCs) have attracted intensive attention in the photovoltaics research community because of its advantages in lightweight, flexibility and low cost, which are critical for future large-area, portable, flexible and wearable applications.[1-4] To date, the power conversion efficiency of large sized FOSCs still fall short for commercial requirements.[5] Apart from the inherent chemical and heterojunction structures, one critical reason is the short diffusion length of the excitons generated in the organic active materials.[6, 7] That is, when one using thicker active layer to enhance light absorption, the charge recombination loss in the active materials also increases due to the low charge carrier mobility and more dead-end transport paths, which often leads to lower power conversion efficiency of the device.[8]

An effective way to improve light absorption of FOSCs is to build periodic light-trapping nanostructures in the device for enhancing light scattering or introducing surface plasmon resonances, etc.[9, 10] For example, surface-relief nanostructures were fabricated on the active or buffer layers of the devices by embossing or rubbing, followed by vacuum deposition of top metal electrodes to form metal nanostructures.[11-14] Electrodes can also be made with nanomaterials such as silver nanowires or their blend with electrical conductive polymer materials, which showed ample plasmonic properties in the visible range, to improve the light absorption.[15-18] However, these approaches are difficult to scale-up for practical applications because they require either direct patterning of the organic layers that may significantly deteriorate the device performance and reproducibility, or the usage of expensive noble metal nanomaterials.[19]

In view of those issues, fabricating bottom metal electrodes with nanoscale relief structures on the plastic substrate is recognized as a more promising way for large-scale application, because of its good compatibility with sequential device fabrication and material deposition procedures.[20] To date, this has been demonstrated by vacuum deposition of a thin metal layer on pre-patterned plastic substrates.[21, 22] Although the

vacuum deposition technique allows the conformal coating of the metal on the surface relief, it is difficult to integrate with roll to roll (R2R) production that are proposed for FOSCs manufacture by the industry. Ideally, the surface-relief bottom electrodes should be fabricated in a solution processible manner such as printing and casting at low temperature, which turns out to be very challenging to achieve. For example, conventional nanoparticle inks, which are mostly reported for printed electronics, are found to be difficult to form the metal coating conformally on the three-dimensional nanoreliefs, because of its high roughness and nanoparticle segregation. To the best of my knowledge, there is no published work on solution fabrication of nanorelief bottom electrodes for FOSCs.

Recently, we develop a solution-processed approach, namely polymer-assisted metal deposition (PAMD), for the fabrication of metal conductors at low temperature.[23-26] PAMD makes use of a thin interfacial polymer, which is chemically modified on targeted polymer substrates, to introduce electroless deposition (ELD) of metal, e.g. Cu, at room temperature in the air. It has been demonstrated that PAMD is very suitable for making smooth, highly adhesive, highly conductive, and flexible metal electrodes on flat plastic substrates for flexible devices such as OSCs and supercapcitors. [27-29]

In this paper, we report the first example of solution printing of light-trapping Cu bottom electrodes on polyethylene terephthalate (PET) with PAMD, which shows remarkable flexibility and significant improvement of the efficiency of full solution-processed FOSCs. FOSCs with these solution-processed nanorelief electrodes present a 13.8% higher short circuit current density (J_{sc}) compared with that of control devices, which leads to a 13.5% enhancement in the power conversion efficiency (PCE) of the device. In addition, the light absorption at low incident angels is also enhanced due to the improved light diffraction from the nanorelief electrodes. More importantly, FOSCs based on these printed nanorelief Cu electrodes also possess remarkable flexibility compared with those made with vacuum evaporation.

2. Experiment section

2.1 Fabrication of printed nanorelief bottom Cu electrodes

175 μm transparent PET film with embossed the hexagonal pillars, which were made by nanoimprinting lithography, was used as the flexible substrate. Substrates was cleaned with detergent, acetone and ethanol in sequence, and dried by clean compress air. Subsequently, they were treated with oxygen plasma for 4 min (Harrick plasma cleaner, model of PDC-32G-2), and immersed into a 0.5wt % [3-(methacryloyloxy)propyl] trimethoxysilane solution (solvent: 95% ethenol, 1% acetic acid) for 1 hour, followed by rinsing. Then these substrates were immersed in an aqueous solution of 2-(methacryloyloxy)ethyl-trimethylammonium chloride (METAC, 20 wt%) and potassiumperoxodisulfate (2.5 g/L), and heated at 60 °C for 60 min for polymerization. Screen printing of catalytic ink ($(NH_4)_2PdCl_4$, (23 mg), PEG (5 g, MW=4000 g/mol) and deionised water (2.3 g)) was performed on the PMETAC-modified substrates to form the ink patterns. The ink-patterned substrates were placed in the dark for 30 min to load $PdCl_4^{2-}$ by ion exchange, followed by treating with plasma for 2 min and rinsing with DI water to remove the ink completely. Finally, The electroless deposition (ELD) of Cu was performed in a plating bath consisting of a 1:1 mixture of freshly prepared solution A and B. Solution A contains NaOH (12 g/L), $CuSO_4 \cdot 5H_2O$ (13 g/L), and potassium sodium tartrate (29 g/L) in DI water. Solution B is a formaldehyde (45 mL/L) aqueous solution. After 5 min deposition, the samples was rinsed by DI water and dried by clean compress air, then transferred to glove box for the following device fabrication.

2.2 Fabrication of FOSCs

The device structure was depicted as Figure 1(a). 70 nm thick printed Cu electrodes on PET were prepared as described above. As control, Cu electrodes made with thermal

evaporation (70 nm) were fabricated on unmodified PET = through a shadow mask at a rate of 0.3 nm/s. Polyethylenimine (PEI) as the electron transport layer (ETL) was spin-coated from its 0.5 wt% 2-methoxyethanol solution onto the Cu electrodes at 5000 rpm for 60 s in a nitrogen-filled glove box, followed by annealing at 100 °C for 10 min. Then, the active layer was spin-coated on PEI at 800 rpm for 60 s in the glove box from the chlorobenzene solution of poly(3-hexylthiophene) (P3HT)/[6,6]-phenyl C61 butyric acid methylester ($PC_{61}BM$) (10:8 in weight ratio), followed by annealing at 145 °C for 5 min to form a 150 nm thick film. Finally, doped highly conductive poly(3,4-ethylenedioxythiophene) polystyrene sulfonate (PEDOT:PSS， denoted herein as PH1000) was spin-coated on the active layer at 1000 rpm for 60 s as transparent top electrode, followed by annealing at 130 °C for 20 min in the glove box to finish the device fabrication. The devices showed different diffraction colors (Figure 1(b) and (c)) at different viewing angles, which indicates the optical diffraction phenomena from the nanorelief Cu electrodes

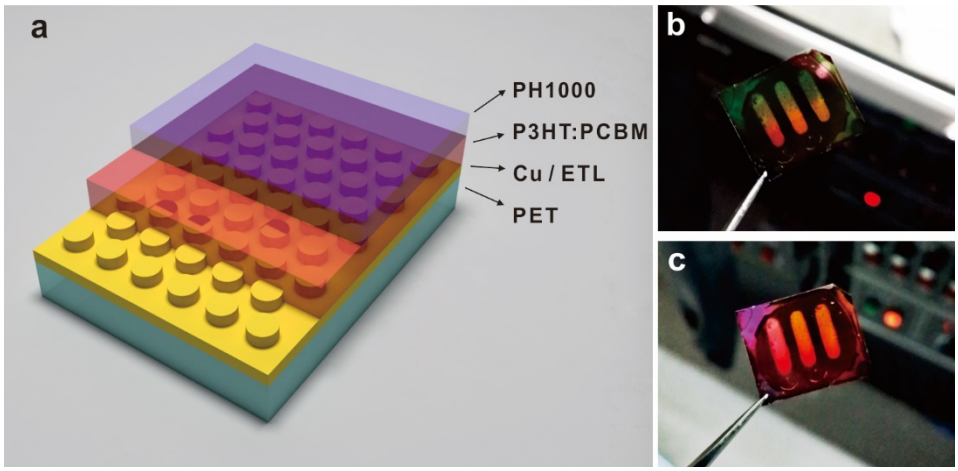

Figure 1. (a) Schematic illustration of the device structure: nanorelief Cu electrodes/ PEI/ P3HT:PCBM/ PH1000. (b, c) Fabricated devices observed at different viewing angles, which showed different diffraction colors.

2.2 Characterization methods

Atomic force microscopy (AFM) was performed with XE-100 (Park System) by non-contact mode. A Keithley 2400 source meter was used to measure the current density-voltage (*J–V*) characteristics of the solar cells, and a 300 W Oriel solar simulator (91160, Newport, 100mW/cm^2, equipped with AM1.5filter) calibrated by a standard silicon solar cell was used as the light source. The external quantum efficiencies (EQEs) of the devices were measured with a standard system equipped with axenon lamp (Oriel 66902, 300W), a monochrometor (Newport66902), a Si detector (Oriel 76175 71580) and a dual channel power meter (Newport 2931 C).

3. Results and discussion

3.1 Characteristics of printed nanorelief bottom Cu electrodes

AFM was firstly used to characterized the surface morphology of the printed nanoreliefs Cu electrodes during their fabrication process. The PET substrate showed nanopillar morphology, with an average height of ~75 nm, width of 500 nm, and pitch of 700 nm (Figure 2a). These nanostructures were uniform over the entire PET substrate (~4 inch) and no significant defect was found (Figure S1), which is beneficial to print high-quality Cu electrodes and to achieve high device performance and stability. After the oxygen plasma treatment, these organic nanopillars were etched slightly, showing a decrease of pillar width to ~350 nm and a rougher surface morphology (Figure 2b). When PMETAC was grown on these nanoreliefs, the surface became much smooth, indicating the dense coating of the polymer brushes (Figure 2c). After the catalytic printing and ELD, the final printed Cu electrode reserved well the nanopillar morphology, showing a final pillar height of ~75 nm and width of ~400 nm (Figure 2d).

Importantly, the pillar height and the nanorelief morphology showed very little change during the electrode fabrication, which indicates that the Cu layer fabricated by PAMD was uniformly and conformably deposited on the PET substrate. In our experiment, the surface roughness of the Cu electrodes as measured on the flat part of the same PET substrate was approximately 6 nm. Even though the entire fabrication was carried out in the air at room temperature, the surface resistance of this 70 nm thick nanoreliefs Cu

electrode was <0.1 ohm/sq. This is a significant advantage of the PAMD fabrication process over the conventional nanoparticle ink method, which often requires a much thicker metal layer (typically >1 μm thick) to achieve low resistance. Those thick metal layers would inevitably submerge the nanorelief structures and make the electrode surface very rough. [30, 31]

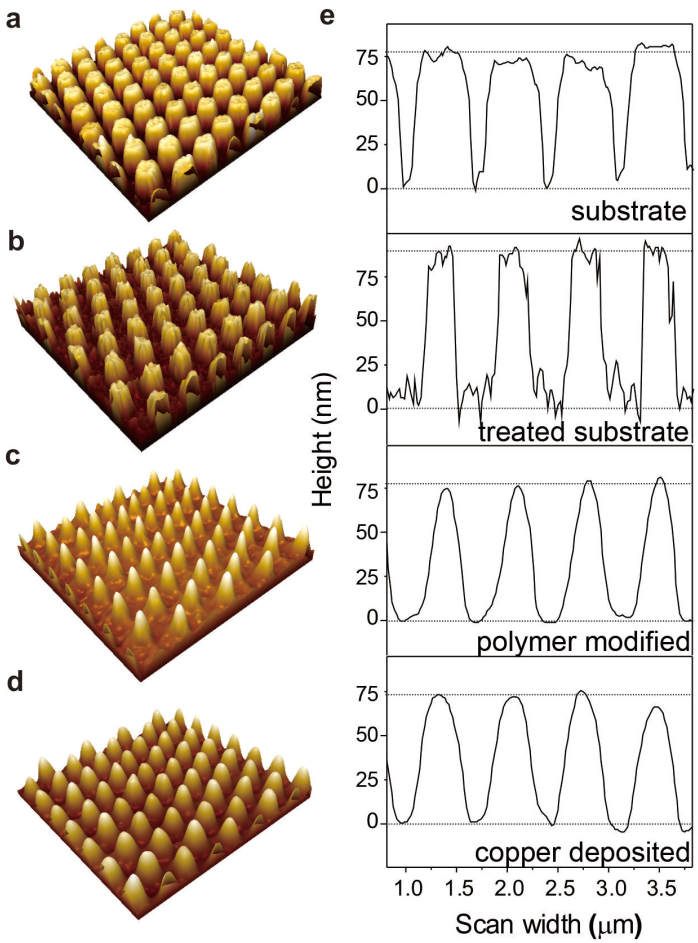

Figure 2. Surface morphology monitoring of the substrate during the solution fabrication of nanorelief Cu electrodes. (a)~(d) are the 3D AFM topographical images of PET substrate before (a) and after (d) oxygen treatment, after PMETAC modification (c) and after Cu deposition (d) (figure size: 5 μm × 5 μm). (e) is the cross section analysis.

3.2 FOSC performance and optical simulation

Device performances were characterized through *J-V* curves and *EQE* spectra. As shown in Figure 3a and Table 1, FOSCs made with nanorelief Cu electrodes had 13.8% higher J_{sc} (7.05 mA/cm^2) than the control devices made with flat Cu electrodes (6.19 mA/cm^2).

This led to 13.5% enhancement in PCE from 1.92% to 2.18% (an average from 20 devices, 5% standard deviation). The enhancement was attributed to two main aspects. (1) The nanorelief Cu electrodes could diffract light, which led to the increase in the optical path of incident light in the active layer, and resulted in enhanced coupling of light power inside the active layer.[32] This can be reflected directly by the increased J_{sc} and and improved *EQE* over the entire optical spectrum. Meanwhile, the open circuit voltage (V_{oc}) and fill factor (FF) were both close to those of control devices, which implied no deflection in the interface to cause recombination losses and carriers transport barriers. (2) The nanorelief structures in the Cu layer also significantly increased the interfacial areas between the cathode and the active layer to improve electron extraction efficiency.[33] This could be proved qualitatively by *J-V* curves of the electron-only device as shown in Figure 4 (c), where the output current densities of the FOSCs with nanoreliefs Cu electrodes were significantly higher than that of the reference ones.

Another important aspect for solar cells is the angular dependent photo response. It should be noted that some expensive inorganic solar cells, such as single crystal Si solar cells, are equipped with mechanical rotating systems to optimize the light incident angles along with the sunlight during the day time. While for the low-cost thin film OSCs, especially for some portable device application, the incident angle of the light varies significantly during the day. Therefore, it is very important to improve the light absorption of the device at low incident angles. The Angular photo response was tested from by varying the incident angle from -70^{o} to 70^{o} (normal incident was set as 0^{o}, Figure 4). It was observed that FOSCs with nanorelief Cu electrodes had higher photocurrent density. This result proved the light trapping strategy not only worked on the vertical incident situation, but also showed absorption enhancement at other incident angles.

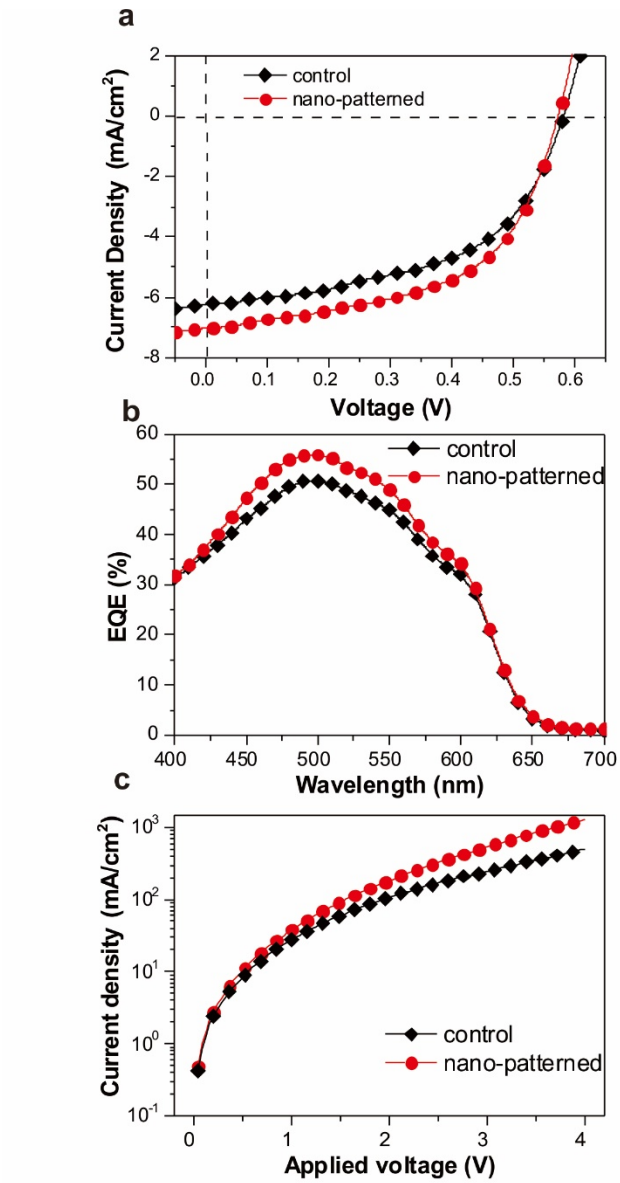

Figure 3. Device performance comparison between those with flat (denoated as control) and nanorelief (denoted as nano-patterned) Cu electrodes, including (a) *J-V* characteristics for power conversion performance; (b) EQE spectrum under illumination with different light wavelength; and (c) *J-V* characteristics of electron-only device for evaluation of the electron mobility.

Table 1. Basic photovoltaic parameters comparison between the devices with flat and nano-patterned printable electrodes.

Electrode configuration	J_{sc}(mA/cm2)	Voc(V)	FF	PCE(%)
flat Cu electrodes	6.19	0.58	0.53	1.9
nanorelief Cu electrodes	7.05	0.57	0.54	2.2

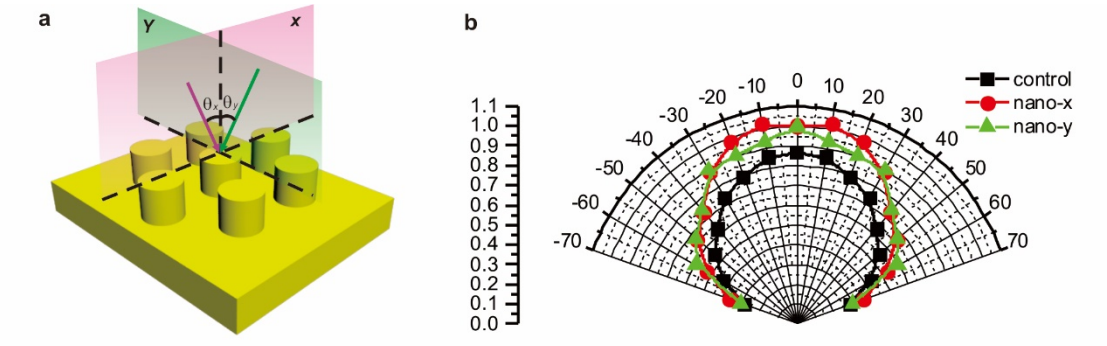

Figure 4. (a) The schematic illustration showing the incident angles for different incident planes in a FOSC with nanorelief Cu electrode; (b) The normalized angular dependent photocurrents of the FOSC with flat and nanorelief electrodes.

On the other hand, optical simulation was carried out to deeper understand the relationship between the nanostructures of Cu electrodes and the absorption enhancement. Finite difference time domain (FDTD) method was taken to build the optical model and run the simulation. Herein, the key parameter was the electrical field density (Q) that can reflect the energy flow dissipation per second for single wavelength in the active layer. The value of Q can be expressed as:

$$Q = \frac{1}{2}\omega\varepsilon'\varepsilon_0 \left|E(\lambda)\right|^2 (1)$$

where ω is the angular frequency the electromagnetic field, ε_0 is the electric permittivity of free space, iε' is the imaginary part of the dielectric function, and λ is the wavelength of light. It was defined that the light polarization direction in the plane x and y (as depicted in Figure 5) corresponded to the S and P polarization, respectively. The simulated horizontal cross section plane was located 35 nm above the surface of PEI layer, and 550 nm was chosen as the simulated wavelength. In the simulated electrical field distribution image (Figure 5), the purple circles refer to the Cu coated nanopillars, around which was the active layer.

From the simulated image, it was observed that enhanced field intensity appeared between two adjacent nanopillars or surrounding the nanopillars. Strong metallic grating resonant enhancement of electrical field could be found between the Cu nanopillars in both

polarization modes. The normalized $|E|^2$ was able to reach more than 0.7, whereas that of the control device with flat structure was only ~0.45. This electrical field density difference could be recognized as the main reason of improvement in the device absorption.

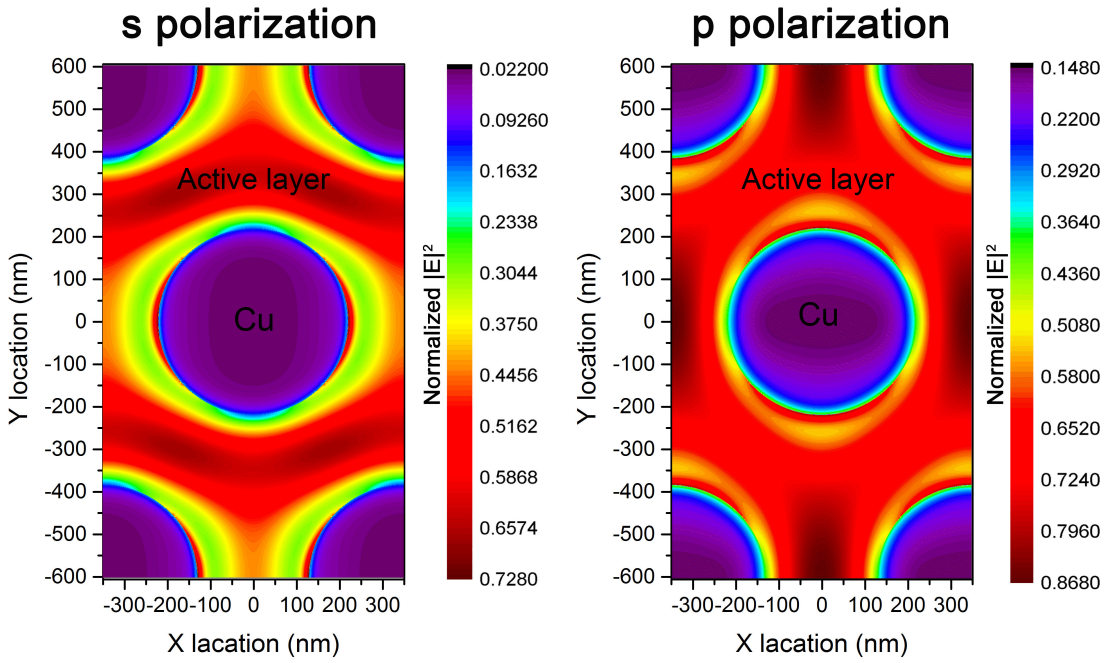

Figure 5. FDTD optical simulation of FOSCs with nanoreliefs Cu electrodes. The results are the horizontal cross section in the device (35 nm above the PEI layer) to show the electrical field distribution under S and P polarization mode.

3.3 Flexibility of FOSCs

Good flexibility of OSCs is highly desirable for a wide variety of flexible, portable, and wearable applications. There already have been a large amount of efforts to improve the flexibility of FOSCs, among which flexible electrodes are the key issues. In our PAMD fabrication approach, the PMETAC layer between Cu and the PET substrate provides remarkable adhesion to Cu layer and improve the flexibility of electrodes. Bending fatigue tests for Cu electrodes and FOSCs were both carried out with a small bending radio of 6.5 mm at a high bending speed of 0.5 Hz. The bending cycles were as many as 500, and each cycle involved one stretching and one compress bending. As reference, nanorelief Cu electrodes fabricated by thermal evaporation of Cu layer on the same

pre-structured PET substrate was fabricated and tested.

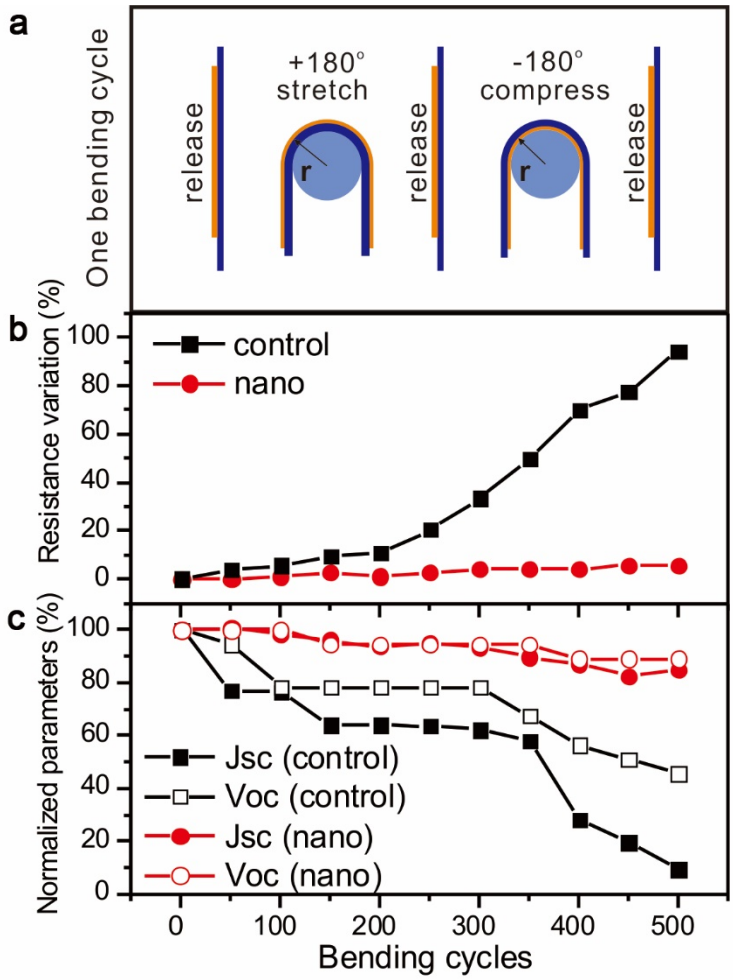

Figure 6. Bending tests of FOSCs made by the printed and evaporated nanorelief Cu electrodes. (a) Illustartion of the the bending test. (b) Resistance variation of Cu electrdoes and (c) performance of FOSCs during 500 cycles of bending tests.

For the Cu electrodes, resistance variation was applied for evaluation. After 500 bending cycles, the resistance of reference samples increased by 100%, but our solution-printed Cu electrodes showed only <5% change. Such a resistance variation is even lower when compared with our previous work on the flat electrode. It can be explained by the fact that nanorelief structures will slow down the electrical conductivity degradation under deformation stress by hindering the crack propagation, if any.[34] More importantly, the

OSCs with printed electrodes also show remarkable flexibility. Two main parameters, J_{sc} and V_{oc}, of the devices were recorded during the bending fatigue tests. For the device with evaporated electrodes, the bending damage to the devices is drastic. The V_{oc} dropped to below half of the initial value, and only 5% of initial J_{sc} can be extracted after 500 bending cycles. In contrast, there was slight decrease, only ~10% both of J_{sc} and V_{oc} in our devices with printed Cu electrodes.

4. Conclusion

For the first time, we reported the solution-printing of nanorelief Cu electrodes on flexible PET substrate in the air at room temperature, which were used as bottom back electrodes for FOSCs. The nanorelief structures on these electrodes improved the photovoltaic performance significantly by 13.5% because of the light scattering effects, which resulted in improved light absorption in the active layer and enhanced contact surface area between the electrode and the active materials. More importantly, the printed Cu electrodes possessed remarkable stability upon mechanical deformation compared with the thermally evaporated ones, and which led to significant improvement of the bending fatigue of the FOSCs under small bending radius (6.5 mm). Importantly, the entire device fabrication is solution-processed, which is compatible with large-area R2R fabrication. Therefore it shows great advantage in cost effectiveness due to the use of low-cost Cu electrode and the removal of vacuum deposition steps.

Acknowledgement

This work was financial supported by GRF of Hong Kong (PolyU 5030/12P and PolyU 5036/13P) and The Hong Kong Polytechnic University (G-UB56).

Reference

[1] M. Zbiri, L. A. Haverkate, G. J. Kearley, M. R. Johnson, F. M. Mulder, in *Neutron Applications in Materials for Energy*, Springer, **2015**, 109.
[2] H. Hoppe, N. S. Sariciftci, *J. Mater. Res.* **2004**, *19*, 1924.
[3] C. Lungenschmied, G. Dennler, H. Neugebauer, S. N. Sariciftci, M. Glatthaar, T. Meyer, A. Meyer, *Solar Energy Materials and Solar Cells* **2007**, *91*, 379.
[4] M. Kaltenbrunner, M. S. White, E. D. Głowacki, T. Sekitani, T. Someya, N. S.

Sariciftci, S. Bauer, *Nature communications* **2012**, *3*, 770.
[5] F. C. Krebs, T. Tromholt, M. Jørgensen, *Nanoscale* **2010**, *2*, 873.
[6] P. E. Shaw, A. Ruseckas, I. D. Samuel, *Adv. Mater.* **2008**, *20*, 3516.
[7] S. R. Forrest, *MRS Bull.* **2005**, *30*, 28.
[8] C. Deibel, A. Wagenpfahl, V. Dyakonov, *physica status solidi (RRL)-Rapid Research Letters* **2008**, *2*, 175.
[9] M. Niggemann, M. Riede, A. Gombert, K. Leo, *physica status solidi (a)* **2008**, *205*, 2862.
[10] D.-H. Ko, J. R. Tumbleston, A. Gadisa, M. Aryal, Y. Liu, R. Lopez, E. T. Samulski, *J. Mater. Chem.* **2011**, *21*, 16293.
[11] S. I. Na, S. S. Kim, J. Jo, S. H. Oh, J. Kim, D. Y. Kim, *Adv. Funct. Mater.* **2008**, *18*, 3956.
[12] C. Battaglia, J. Escarré, K. Söderström, M. Charrière, M. Despeisse, F.-J. Haug, C. Ballif, *Nature Photonics* **2011**, *5*, 535.
[13] K. Li, H. Zhen, Z. Huang, G. Li, X. Liu, *ACS applied materials & interfaces* **2012**, *4*, 4393.
[14] W. C. H. Choy, X. Ren, *IEEE Journal of Selected Topics in Quantum Electronics* **2015**, *22*, 1.
[15] M. G. Kang, T. Xu, H. J. Park, X. Luo, L. J. Guo, *Advanced Materials* **2010**, *22*, 4378.
[16] B. Y. Wang, T. H. Yoo, W. L. Ju, B. I. Sang, D. S. Lim, W. K. Choi, D. K. Hwang, Y. J. Oh, *Small* **2015**, *11*, 1905.
[17] H. Tan, R. Santbergen, A. H. M. Smets, M. Zeman, *Nano Lett.* **2012**, *12*, 4070.
[18] S. Shahin, P. Gangopadhyay, R. A. Norwood, *Appl. Phys. Lett.* **2012**, *101*, 6335.
[19] G. Garcia-Belmonte, A. Munar, E. M. Barea, J. Bisquert, I. Ugarte, R. Pacios, *Org. Electron.* **2008**, *9*, 847.
[20] A. Mihi, F. J. Beck, T. Lasanta, A. K. Rath, G. Konstantatos, *Adv. Mater.* **2014**, *26*, 443.
[21] R. Søndergaard, M. Hösel, D. Angmo, T. T. Larsen-Olsen, F. C. Krebs, *Mater. Today* **2012**, *15*, 36.
[22] F. C. Krebs, S. A. Gevorgyan, J. Alstrup, *Journal Of Materials Chemistry* **2009**, *19*, 5442.
[23] X. Liu, H. Chang, Y. Li, W. T. Huck, Z. Zheng, *ACS applied materials & interfaces* **2010**, *2*, 529.
[24] X. Wang, H. Hu, Y. Shen, X. Zhou, Z. Zheng, *Advanced Materials* **2011**, *23*, 3090.
[25] R. Guo, Y. Yu, Z. Xie, X. Liu, X. Zhou, Y. Gao, Z. Liu, F. Zhou, Y. Yang, Z. Zheng, *Advanced Materials* **2013**, *25*, 3343.
[26] Y. Yu, C. Yan, Z. Zheng, *Advanced Materials* **2014**, *26*, 5508.
[27] K. Li, H. Zhen, L. Niu, X. Fang, Y. Zhang, R. Guo, Y. Yu, F. Yan, H. Li, Z. Zheng, *Adv. Mater.* **2014**, *26*, 7271.
[28] L. Liu, Y. Yu, C. Yan, K. Li, Z. Zheng, *Nature communications* **2015**, *6*.
[29] Q. Huang, L. Liu, D. Wang, J. Liu, Z. Huang, Z. Zheng, *Journal of Materials Chemistry A* **2016**.
[30] H. F. Dam, F. C. Krebs, *Sol. Energy Mater. Sol. Cells* **2012**, *97*, 191.

[31]B. Y. Ahn, E. B. Duoss, M. J. Motala, X. Guo, S.-I. Park, Y. Xiong, J. Yoon, R. G. Nuzzo, J. A. Rogers, J. A. Lewis, *Science* **2009**, *323*, 1590.
[32]J. You, X. Li, F. x. Xie, W. E. Sha, J. H. Kwong, G. Li, W. C. Choy, Y. Yang, *Advanced Energy Materials* **2012**, *2*, 1203.
[33]M. G. Deceglie, V. E. Ferry, A. P. Alivisatos, H. A. Atwater, *Nano Lett.* **2012**, *12*, 2894.
[34]R. Guo, Y. Yu, J. Zeng, X. Liu, X. Zhou, L. Niu, T. Gao, K. Li, Y. Yang, F. Zhou, *Advanced Science* **2015**, *2*.

Supporting Information

Printed light-trapping nanorelief Cu electrodes for full-solution-processed flexible organic solar cells

Kan Li[1,2], Yaokang Zhang[1,3], Hongyu Zhen[1,2], Liyong Niu[1,3], Xu Fang[2], Zhike Liu[4], Weidong Shen[2], Haifeng Li[2] and Zijian Zheng[1,3,*]

Dr. Kan Li, Mr. Yaokang Zhang, Dr. Hongyu Zhen, Mr. Liyong Niu, Prof. Zijian Zheng

5. Nanotechnology Center, Institute of Textiles and Clothing, the Hong Kong Polytechnic University, Hong Kong, China

E-mail: tczzheng@polyu.edu.hk

Dr. Kan Li, Dr. Hongyu Zhen, Mr. Xu Fang, Prof. Weidong Shen, Prof. Haifeng Li

6. State Key laboratory of modern optical instrumentation, Zhejiang University, 38# Zheda Road,Hangzhou 310027, P.R.China,

Mr. Yaokang Zhang, Mr Liyong Niu, Prof. Zijian Zheng

7. Advanced Research Centre for Fashion and Textiles, the Hong Kong Polytechnic University Shenzhen Research Institute, Shenzhen 518000, China

Dr. Zhike Liu

8. Department of Applied Physics, the Hong Kong Polytechnic University, Hong Kong, China

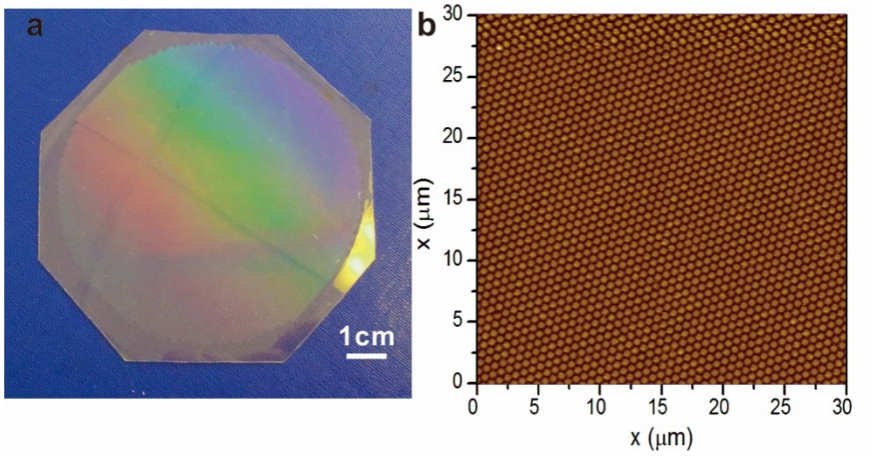

Figure S1 (a) Optical image of the PET substrate with pre-patterned nanopillar structures. (b) AFM image of the PET substrate (30 μm × 30 μm).